R center in KCl. II. Line-shape calculation of the R_2 band*

Gary G. DeLeo,† Richard C. Kern,‡ and Ralph H. Bartram
Department of Physics, University of Connecticut, Storrs, Connecticut 06268
(Received 24 November 1980)

The optical-absorption properties of the R center in KCl are investigated theoretically. The single-phonon-sideband line shapes associated with the creation of A_1- and E-symmetry phonons are simulated for the R_2 band, where self-consistent-field molecular-orbital point-ion-model wave functions are employed. The electron-lattice interaction is treated in two approximations: a Ritter and Markham approach appropriate to relatively diffuse wave functions, and a Green's-function approach appropriate to relatively compact wave functions. The Green's-function method admits a treatment of perturbed-lattice dynamics although such an extension is not possible in the Ritter and Markham approach. The Green's-function method appropriate to the perfect-lattice spectrum gives results which most closely agree with experiment. The calculated line shapes, Huang-Rhys factors, and effective Jahn-Teller coupling constants and frequencies are presented.

I. INTRODUCTION

In the van Doorn[1] model for the R center, three electrons are trapped at the sites of three anion vacancies forming an equilateral triangle in the (111) plane. In the preceding article[2] (hereafter referred to as I), we treated the electronic structure and the magneto-optical parameters associated with the ground electronic state of the R center in KCl. The electronic structure was calculated using molecular-orbital theory with configuration mixing appropriate to a point-ion potential. The excited electronic states were correlated with the observed optical-absorption bands. The dominant configuration of the ground electronic state was employed in a calculation of the magneto-optical parameters: spin-orbit constant and orbital g value. A comparison was made with these parameters as inferred from electron-spin resonance (ESR) and magnetic circular dichroism (MCD). In the present investigation, we return to the optical-absorption properties and consider the structure observed in the R_2 absorption band. It is well known that this structure arises as a consequence of the electron-lattice interaction.[3]

The R_2 band is of particular interest since it exhibits a zero-phonon line and attendant multiphonon structure. Giesecke *et al.*[4] have developed a procedure for deconvoluting line shapes into n-phonon contributions when the center exhibits relatively weak electron-lattice coupling. They have applied this procedure to the R center in KCl, generating the single-phonon-sideband line shape and the multiphonon contributions. Only the single-phonon sideband need be considered since the others may be developed from this.[5] In the present investigation, the multiconfigurational wave functions from I, corresponding to the lowest $^2A_2$ and ^2E states, are employed in a calculation of the single-phonon-sideband line shape. This line shape is associated with the R_2 optical-absorption band and is compared with the empirical line shape inferred by Giesecke *et al.*[4]

The calculation of line shapes requires a treatment of the defect electronic structure, the crystal-lattice dynamics, and the electron-lattice interaction. The electronic structure was discussed in I. The breathing-shell model[6] is assumed to provide an adequate description of the dynamics of the perfect lattice. The theory of line shapes, which incorporates the electron-lattice interaction, is developed for linear coupling within the framework of the adiabatic approximation, following the formulation of O'Rourke.[7] This treatment is appropriate only when either the electronic states or the normal modes of vibration are nondegenerate. Since the defect has C_{3v} symmetry, electronic states and vibrational modes must transform according to the A_1, A_2, or E irreducible representations. The treatment described above is appropriate to the absorption of photons accompanied by the creation of A_1-symmetry phonons. This theory is extended by employing the method of O'Brien[8] to include coupling to the degenerate E vibrational modes. The coupling of the ^2E ground state to the E modes of vibration gives rise to a dynamic Jahn-Teller effect.[9,10]

The electron-lattice interaction is treated in two approximations: a Ritter and Markham[11] approach appropriate to relatively diffuse wave functions, and a Green's-function approach[12,13] appropriate to relatively compact wave functions. In the first approach, the lattice spectrum is assumed to be unaltered by the presence of the defect and the electron-lattice potential is effectively averaged over each unit cell. The Green's-function approach is not limited to perfect-lattice dynamics and the electron-lattice potential is not averaged. The interaction is, however, restricted for practical reasons to a finite set of ions surrounding

the geometrical center of the defect.

The theory of lattice dynamics is described in Sec. II. The theory of line shapes is presented in Sec. III. The methods used in evaluating line shapes in the diffuse- and compact-wave-function approximations are considered in Secs. IV and V, respectively. These procedures are applied to the R center in KCl and the results are compared with experiment. A summary of results and discussion is presented in Sec. VI.

II. THEORY OF LATTICE DYNAMICS

A. Perfect lattice

In the harmonic approximation, the Hamiltonian for the perfect point-ion (no atomic polarization) solid is[13]

$$H = \tfrac{1}{2}\underline{p}^{\dagger}\underline{M}^{0}\underline{p} + \tfrac{1}{2}\underline{u}^{\dagger}\underline{\Phi}^{0}\underline{u}\,. \tag{1}$$

The vectors $\underline{u}$ and $\underline{p}$ represent displacements from equilibrium and conjugate momenta, respectively. The elements of the vectors are labeled $l\kappa\alpha$, where l denotes the lattice site, κ the ion type, and α the direction of displacement (x,y,z). $\underline{M}^{0}$ is a diagonal matrix containing the ion masses and $\underline{\Phi}^{0}$ is the force-constant matrix. If the displacements are assumed to have a time dependence of the form $e^{-i\omega t}$, then the amplitudes satisfy

$$\underline{L}^{0}(\omega^{2})\underline{u} = 0\,, \tag{2}$$

where $L^{0}(\omega^{2})$ is defined for the perfect lattice by

$$\underline{L}^{0}(\omega^{2}) \equiv \underline{M}^{0}\omega^{2} - \underline{\Phi}^{0}\,. \tag{3}$$

The set of eigenvalues ω_j^2 and eigenvectors $\underline{\chi}_j^0$ resulting from the solution of this set of equations satisfy orthonormality and closure relations of the form

$$\underline{\chi}_j^{0\dagger}\underline{M}^{0}\underline{\chi}_{j'}^{0} = \delta_{jj'} \tag{4}$$

and

$$\sum_j \underline{M}^{0}\underline{\chi}_j^{0}\underline{\chi}_j^{0\dagger} = \underline{I}\,. \tag{5}$$

The motion of the perfect lattice is completely determined by the matrix $\underline{L}^{0}(\omega^{2})$ and a set of initial conditions. The perfect-lattice Green's-function matrix, which is defined as the inverse of the matrix $\underline{L}^{0}(\omega^{2})$, may be expressed in terms of the lattice eigenmodes,

$$\underline{G}^{0}(\omega^{2}) = \sum_j \frac{\underline{\chi}_j^{0}\underline{\chi}_j^{0\dagger}}{\omega^{2} - \omega_j^{2}}\,. \tag{6}$$

According to Bloch's theorem, the eigenvectors of the perfect lattice may be expressed in terms of the polarization vectors, $e_\alpha(\kappa;\vec{k}j)$, as

$$\chi_{\vec{k}j}^{0}(l\kappa\alpha) = N^{-1/2} e_\alpha(\kappa;\vec{k}j)\exp[i\vec{k}\cdot\vec{x}(l\kappa)]\,, \tag{7}$$

where the $\vec{k}j$ pair now replaces j. The displacement vector between an arbitrary origin and ion $l\kappa$ is denoted $\vec{x}(l\kappa)$; the wave vector and branch index are $\vec{k}$ and j, respectively; the number of unit cells and therefore the number of wave vectors in the first Brillouin zone is N. The polarization vectors satisfy

$$M_\kappa^{0}\omega_{\vec{k}j}^{2} e_\alpha(\kappa;\vec{k}j) = \sum_{\kappa'\beta} D(\kappa\alpha;\kappa'\beta\,|\,\vec{k}) e_\beta(\kappa';\vec{k}j)\,, \tag{8}$$

where $D(\vec{k})$ is the Fourier-transformed dynamical matrix with elements given by

$$D(\kappa\alpha;\kappa'\beta\,|\,\vec{k}) = \sum_{l'} \Phi_{l\kappa\alpha;l'\kappa'\beta}\exp\{-i\vec{k}\cdot[\vec{x}(l\kappa) - \vec{x}(l'\kappa')]\}\,, \tag{9}$$

A more useful form of the Green's function results from its continuation onto the complex plane. In the limit as ϵ goes to zero, the real and imaginary parts become

$$\mathrm{Re}\underline{G}^{0}(\omega^{2} - i\epsilon) = \pi^{-1}\mathrm{P}\int_0^{\omega_{\max}} \mathrm{Im}\underline{G}^{0}(\omega'^{2} - i\epsilon)\frac{2\omega' d\omega'}{\omega^{2} - \omega'^{2}} \tag{10}$$

and

$$\mathrm{Im}\underline{G}^{0}(\omega^{2} - i\epsilon) = \frac{\pi}{2\omega}\sum_j \underline{\chi}_j^{0}\underline{\chi}_j^{0\dagger}\delta(\omega - \omega_j)\,. \tag{11}$$

The symbol P denotes the Cauchy principal value and $\omega_{\max}$ is the maximum lattice frequency.

The point-ion treatment described above ignores the effects of atomic polarizability which are known to be important in ionic solids, particularly for the longitudinal vibrations. A shell model, developed by Dick and Overhauser,[14] separates each ion into a massive core and a massless shell. The displacement of the shell relative to the core gives rise to atomic polarization. The shells are connected to the cores by strong isotropic springs in this model. A refinement of the shell model to incorporate atomic dilatations is due to Schröder.[6] This is the breathing-shell model for lattice dynamics. In this model, Eq. (8) is replaced by the set of equations

$$M^{0}\omega_{\vec{k}j}^{2} e^{C}(\vec{k}j) = [R(\vec{k}) + R'(\vec{k}) + ZC(\vec{k})Z]e^{C}(\vec{k}j) + [R(\vec{k}) + ZC(\vec{k})Y]e^{S}(\vec{k}j) + Q(\vec{k})e^{B}(\vec{k}j)\,, \tag{12a}$$

$$0 = [R(\vec{k})^{\dagger} + YC(\vec{k})Z]e^{C}(\vec{k}j) + [R(\vec{k}) + G + YC(\vec{k})Y]e^{S}(\vec{k}j) + Q(\vec{k})e^{B}(\vec{k}j)\,, \tag{12b}$$

and

$$0 = Q(\vec{k})^{\dagger}[e^{C}(\vec{k}j) + e^{S}(\vec{k}j)] + H(\vec{k})e^{B}(\vec{k}j), \qquad (12c)$$

where $e^{C}(\vec{k}j)$ and $e^{S}(\vec{k}j)$ are the core and shell (measured relative to the core) polarization vectors and $e^{B}(\vec{k}j)$ has two components describing the dilatations of cation and anion shells. The $C(\vec{k})$ matrix incorporates the electrostatic interactions, M^{0} is a mass matrix, Z is an ionic-charge matrix, and Y is a shell-charge matrix. The symbol G denotes the diagonal matrix which represents the isotropic core-shell force constants. The other matrices are associated with short-range repulsive interactions.

Copley *et al.*[15] have solved the breathing-shell-model equations for the perfect KCl lattice. The adjustable parameters were determined by fitting the dispersion curves to those generated from inelastic neutron scattering. We use their model-IV parameters, from which the following are inferred: $G_1 = 965.0$, $G_2 = 480.9$, $Y_1 = 5.758$, and $Y_2 = -4.205$. The G_κ are in units of e^2/v where v is the unit-cell volume and $Z_1 = -Z_2 = 0.928$ are the total ionic charges. We employ this set of parameters in a calculation of the eigenmodes of the perfect KCl lattice using approximately 66 000 wave vectors in the first Brillouin zone.

The perfect-lattice Green's function is extended to accommodate the shell and breathing degrees of freedom. The imaginary part is calculated by averaging over a frequency interval $\Delta\omega$ about ω,

$$\mathrm{Im}G^{0AA'}(l\kappa\alpha; l'\kappa'\beta \,|\, \omega^2 - i\epsilon) = \frac{\pi}{2\omega\Delta\omega N}\sum_{\vec{k}j}{}' e^{A}_{\alpha}(\kappa; \vec{k}j) e^{A'}_{\beta}(\kappa'; \vec{k}j) \times \exp\{i\vec{k}\cdot[\vec{x}(l\kappa) - \vec{x}(l'\kappa')]\}, \qquad (13)$$

where the sum is restricted by $\omega - \frac{1}{2}\Delta\omega \leq \omega_j \leq \omega + \frac{1}{2}\Delta\omega$. As a consequence of cubic symmetry, the sum over $\vec{k}$ is required only for the unique $\frac{1}{48}$ of the first Brillouin zone. Equation (10) for the real part is now replaced by[16]

$$\mathrm{Re}\underline{G}^{0}(\omega^2 - i\epsilon) = \pi^{-1}\mathrm{P}\int_0^{\omega_{\max}} \mathrm{Im}\underline{G}^{0}(\omega'^2 - i\epsilon)\frac{2\omega' d\omega'}{\omega^2 - \omega'^2} + \underline{W}. \qquad (14)$$

In calculating the real part by Eq. (14), the imaginary part is approximated by a series of straight-line segments, and the integral is evaluated exactly within each frequency interval $\Delta\omega$. The frequency-independent matrix $\underline{W}$ is given in terms of the force-constant matrix by[16]

$$\underline{W}^{SS} = -(\underline{\Phi}^{SS} - \underline{\Phi}^{SB}\underline{\Phi}^{BB^{-1}}\underline{\Phi}^{BS}), \qquad (15a)$$

$$\underline{W}^{SB} = -\underline{W}^{SS}\underline{\Phi}^{SB}\underline{\Phi}^{BB^{-1}}, \qquad (15b)$$

$$\underline{W}^{BS} = -\underline{\Phi}^{BB^{-1}}\underline{\Phi}^{BS}\underline{W}^{SS}, \qquad (15c)$$

and

$$\underline{W}^{BB} = -\underline{W}^{BS}\underline{\Phi}^{SB}\underline{\Phi}^{BB^{-1}} - \underline{\Phi}^{BB^{-1}}. \qquad (15d)$$

Products and inverses of very large force-constant matrices are required, but these operations become tractable when performed in reciprocal space.

B. Defect lattice

When a point defect is introduced, the ions surrounding the defect experience static forces tending to move them toward new equilibrium positions. In addition, the force-constant matrix elements which describe the restoring forces are altered. In a point-ion solid, the force on ion $l\kappa$ in direction α is

$$F_{l\kappa\alpha} = -\frac{\partial}{\partial x_{l\kappa\alpha}} V(x), \qquad (16)$$

where $V(x)$ is the adiabatic potential energy. The changes in the force-constant matrix are given by

$$\delta\Phi_{l\kappa\alpha; l'\kappa'\beta} = \frac{\partial^2}{\partial x_{l\kappa\alpha}\partial x_{l'\kappa'\beta}} V(x) - \Phi^{0}_{l\kappa\alpha; l'\kappa'\beta}. \qquad (17)$$

In the present treatment, Eqs. (16) and (17) are evaluated for a breathing-shell model within the framework of the "fully adiabatic" approximation. This means that the shells and cores both follow the averaged positions of the trapped electrons while the shells follow the instantaneous positions of the cores. The adiabatic potential energy may be written as follows:

$$V(x) = V_{II}(x) + (\Psi(r, x), [T_e + V_{ee}(r) + V_{e\phi}(r, x)]\Psi(r, x)). \qquad (18)$$

The set of excess-electron coordinates is denoted by r and the set of core and shell coordinates by x. The kinetic and electron-electron-interaction energies are denoted T and $V_{ee}(r)$, respectively. The term $V_{e\phi}(r, x)$ describes the Coulomb interaction between the excess electrons and the cores and shells. The ion-ion energy is denoted $V_{II}(x)$ and includes a Born-Mayer[17] part and a Coulomb part. The Born-Mayer exponential parameter is chosen as 0.33 Å after Tosi[18] and the pre-exponential factor is chosen so that the second derivative is consistent with the corresponding shell-model parameter.[15] The electronic state is described by the wave function $\Psi(r, x)$, which depends parametrically on the core and shell coordinates.

The dynamics of the lattice containing the defect is described by a perturbed-lattice Green's-function matrix,

$$\underline{G}(\omega^2) \equiv \underline{L}(\omega^2)^{-1}, \tag{19}$$

where

$$\underline{L}(\omega^2) = \underline{M}\omega^2 - \underline{\Phi}. \tag{20}$$

If $\delta\underline{M}$ is taken to represent the change in the mass matrix, then[12]

$$\underline{G}(\omega^2) = [\underline{I} - \underline{G}^0(\omega^2)\delta\underline{L}]^{-1}\underline{G}^0(\omega^2), \tag{21}$$

where

$$\delta\underline{L} \equiv -\delta\underline{M}\omega^2 + \delta\underline{\Phi}. \tag{22}$$

Since the shells are assumed to be massless, Eqs. (12) can be exploited to eliminate the shell and breathing coordinates in favor of the core coordinates. The effective Hamiltonian can then be written in the form

$$H = \tfrac{1}{2}\underline{p}^{C\dagger}\underline{M}^{CC-1}\underline{p}^{C} + \underline{u}^{C\dagger}\underline{\Phi}^{CC'}\underline{u}^{C} - \underline{u}^{C\dagger}\underline{F}^{C'}, \tag{23}$$

where the effective force vector $\underline{F}^{C'}$ and force-constant matrix $\underline{\Phi}^{CC'}$ are given, respectively, by

$$\underline{F}^{C'} = \underline{F}^{C} + (\underline{\Phi}^{CS} - \underline{\Phi}^{CB}\underline{\Phi}^{BB-1}\underline{\Phi}^{BS})\underline{W}^{SS}\underline{F}^{S} \tag{24}$$

and

$$\underline{\Phi}^{CC'} = \underline{\Phi}^{CC} - \underline{\Phi}^{CB}\underline{\Phi}^{BB-1}\underline{\Phi}^{BC} + (\underline{\Phi}^{CS} - \underline{\Phi}^{CB}\underline{\Phi}^{BB-1}\underline{\Phi}^{BS})\underline{W}^{SS}(\underline{\Phi}^{SC} - \underline{\Phi}^{SB}\underline{\Phi}^{BB-1}\underline{\Phi}^{BC}). \tag{25}$$

Equation (24) incorporates the assumption that the defect introduces no force acting directly on the breathing coordinate. It is important to retain the linear terms in Eq. (23), since the equilibrium-lattice conformation depends on the electronic state of the defect. A transformation to normal coordinates Q_j can be effected by expanding $\underline{u}^{C}$ in the form

$$\underline{u}^{C} = \sum_j Q_j \underline{\chi}_j^{C'}, \tag{26}$$

where $\underline{\chi}_j^{C'}$ is an eigenvector of $\underline{\Phi}^{CC'}$. The resulting form for the Hamiltonian, useful for subsequent developments, is

$$H = \sum_j [\tfrac{1}{2}(P_j^2 + \omega_j^2 Q_j^2) + V_j Q_j], \tag{27}$$

where V_j is given by

$$V_j \equiv -\underline{\chi}_j^{C'\dagger}\underline{F}^{C'} = -\underline{\chi}_j^{\dagger}\underline{F}. \tag{28}$$

The second equality is readily demonstrated from Eqs. (24) and (25), and provides an expression for V_j in which shell and breathing coordinates are explicitly retained.

III. THEORY OF LINE SHAPES IN THE LINEAR COUPLING APPROXIMATION

A. Nondegenerate states

A theory of optical line shapes for defects in solids was developed by Huang and Rhys[19] on the basis of the Franck-Condon principle, in which linear coupling to only a single effective mode of vibration was considered. The theory was subsequently reformulated and extended to encompass both linear and quadratic coupling to many modes of different frequencies.[20-24]

The Born-Oppenheimer approximation is assumed in these theories; i.e., the vibronic wave function is written as a product of electronic and vibrational factors:

$$\Psi_{n\nu}(r, Q) \approx \phi_n(r, Q)\chi_{n\nu}(Q). \tag{29}$$

Accordingly, they are strictly applicable only to transitions between nondegenerate electronic states. With the additional assumption of the mean-value and Condon approximations,[20] the absorption coefficient associated with a transition between electronic states a and b is proportional to the normalized line-shape function

$$I_{ba}(E) = \mathrm{Av}_\alpha \sum_\beta |(\chi_{b\beta}, \chi_{a\alpha})|^2 \delta(E_{b\beta} - E_{a\alpha} - E), \tag{30}$$

where Av_α denotes a thermal average over initial vibrational states.

In the case of linear coupling, the Fourier transform of the line-shape function can be expressed as[7]

$$G_{ba}(t) \equiv \int_{-\infty}^{\infty} \exp\left(\frac{iEt}{\hbar}\right) I_{ba}(E)E = \exp[-S + g_1(t)]. \tag{31}$$

The line-shape function can be recovered by inverse Fourier transformation of $G_{ba}(t)$ and can be expressed in terms of n-phonon contributions by expanding $\exp[g_1(t)]$ in a power series[5,12]

$$I_{ba}(E) = e^{-S}\left(\delta(E) + \sum_{n=1}^{\infty} s_n(E)\right). \tag{32}$$

The single-phonon sideband $s_1(E)$ is then

$$s_1(E) = (2\pi\hbar)^{-1}\int_{-\infty}^{\infty} \exp\left(\frac{-iEt}{\hbar}\right) g_1(t)dt, \tag{33}$$

and, from the convolution theorem,[25] $s_n(E)$ satisfies the recursion relation

$$s_n(E) = n^{-1}\int s_1(E_1)s_{n-1}(E - E_1)dE_1. \tag{34}$$

Note that E is measured with respect to the zero-phonon line. The Huang-Rhys factor S and single-phonon sideband $s_1(E)$ are simply related by[11]

$$S = \int s_1(E)dE, \tag{35}$$

and $s_1(E)$ is given, in the limit $T=0$, by

$$s_1(E)=\sum_j S_j\delta(E-\hbar\omega_j). \tag{36}$$

Here, S_j is the per-mode Huang-Rhys factor, related to the coupling constant V_j of Eq. (28) by

$$S_j=|V_j^b-V_j^a|^2/2\hbar\omega_j^3. \tag{37}$$

Giesecke *et al.*[4] have employed Eqs. (31) and (33) to construct $s_1(E)$ at low temperature, with S determined by the relative intensity of the zero-phonon line. Thus the single-phonon sideband $s_1(E)$ provides a suitable point of contact for comparison of theory with experiment.

Although the foregoing theory was derived with the assumption of nondegenerate electronic states, it is applicable to transitions between degenerate states, as well, provided that the coupling is restricted to fully symmetrical modes of vibration which do not mix degenerate states.

B. Dynamic Jahn-Teller effect

The defect normal coordinates and electronic wave functions of the R center in KCl transform like A_1, A_2, or E irreducible representations of point group C_{3v}. Since the ground electronic state has been identified as ^2E, and the R_2 band associated with the transition $^2A_2 \leftarrow {}^2E$,[2,26] it is clear that the line-shape theory described above is applicable only for modes of A_1 symmetry. Coupling of the ^2E state to modes of E symmetry is of particular interest as an example of the dynamic Jahn-Teller effect.[9,10] Although most treatments of the Jahn-Teller effect have employed a cluster model, with coupling to a single set of degenerate modes,[27] the many-mode Jahn-Teller problem has been considered by several investigators.[8,28-34] We have adopted the approach advocated by O'Brien,[8] which is particularly expedient for computation.

The Hamiltonian of Eq. (27) can be generalized to accommodate coupling of degenerate electronic states to degenerate modes of vibration. It may be represented as a matrix within the manifold of degenerate electronic states,

$$H=\sum_j\sum_\gamma[\tfrac{1}{2}(P_j^{(\gamma)2}+\omega_j^2Q_j^{(\gamma)2})I+V_jQ_j^{(\gamma)}U^{(\gamma)}], \tag{38}$$

where γ labels degenerate modes (corresponding to the rows of an irreducible representation), I is the identity matrix, and the $U^{(\gamma)}$ are noncommuting matrices determined solely by symmetry.[35] The coupling constants V_j are still given by Eq. (28), except that $\underline{F}$ is replaced by a vector $-\underline{V}$ whose elements are off-diagonal matrix elements of potential derivatives between degenerate electronic states.

O'Brien[8] employs the Hamiltonian of Eq. (38) in second-quantized form. An orthogonal transformation of the many-mode Hamiltonian is effected, resulting in a new set of creation and annihilation operators, $\alpha_j^\dagger$ and α_j, satisfying the same commutation rules as the usual set. A single effective mode (say, number one) is singled out and coupling to this mode is maximized. In the lowest order of approximation, the many-mode problem is reduced to an effective single-mode problem with effective frequency $\omega_{\rm eff}$ and effective coupling constant $k_{\rm eff}$; hence,

$$H_{\rm eff}=\hbar\omega_{\rm eff}\sum_\gamma[\alpha_1^{\gamma\dagger}\alpha_1^\gamma I+2^{-1/2}k_{\rm eff}(\alpha_1^\gamma+\alpha_1^{\gamma\dagger})U^{(\gamma)}]. \tag{39}$$

The effective coupling constant and effective frequency are given by O'Brien as

$$k_{\rm eff}^2=\hbar^{-1}\sum_j\frac{V_j^2}{\omega_j^3} \tag{40}$$

and

$$\omega_{\rm eff}=\left(\hbar^{-1}\sum_j\frac{V_j^2}{\omega_j^2}\right)\Big/k_{\rm eff}^2. \tag{41}$$

In the present investigation, an estimate is made of the line shape associated with the creation of single E-mode phonons. The effective frequency given by O'Brien's method serves to locate the center of the band with respect to the zero-phonon line. A measure of the intensity of the transition (area under the curve) is determined by $k_{\rm eff}^2/2$. The single effective mode to which the electronic system is coupled is not a true normal mode of the system, but is in turn coupled to other effective modes, with consequent broadening of the absorption band. O'Brien[8] has shown that the application of second-order perturbation theory to the higher-order terms of the Hamiltonian gives a second moment for the band,

$$\langle\omega^2\rangle=\left(\hbar^{-1}\sum_j\frac{V_j^2}{\omega_j}\right)\Big/k_{\rm eff}^2. \tag{42}$$

Optical-absorption bands with distinctive structural features are associated with transitions to degenerate final states.[10,29,30,32] However, bands associated with transitions from degenerate initial states to nondegenerate final states are expected to be relatively featureless in the strong-coupling limit.[10] Accordingly, the first two moments of the band may provide an adequate representation for the contribution of coupling to E modes in the present application.

In the present treatment, it is assumed that the line-shape contributions from A_1 and E modes are independent of each other. This is probably not rigorously true; however, it is assumed to be an adequate approximation. The contribution of

A_2 modes to the line shape has not been considered.

IV. DIFFUSE-WAVE-FUNCTION APPROXIMATION FOR OPTICAL-ABSORPTION CALCULATIONS: RITTER AND MARKHAM APPROACH

Ritter and Markham[11] have developed an approximate form for the electron-lattice interaction potential. Linear electron-lattice coupling was assumed in their model with the lattice spectrum taken to be unaltered by the presence of the defect. A further simplification was introduced by essentially averaging the potential over each unit cell. The detailed structure of the field is neglected; hence, the treatment is most appropriate to diffuse wave functions which remain relatively constant over a unit cell.

The electron-lattice interaction energy derived by Ritter and Markham is given by

$$V_{e\phi}(\vec{r}, Q) = -\sqrt{2}\, i \sum_{\vec{k}j} g_{\vec{k}j} e^{i\vec{k}\cdot\vec{r}} Q_{\vec{k}j}\,, \tag{43}$$

where

$$g_{\vec{k}j} \equiv -\frac{2\pi e^2}{r_0^3}\sqrt{N} \sum_{\kappa} Z_\kappa \vec{k}\cdot\vec{e}(\kappa;\vec{k}j)/|\vec{k}|^2 . \tag{44}$$

The sum in Eq. (43) runs over the branch indices and the N wave vectors of the first Brillouin zone. The Z_κ in Eq. (44) represent the ionic charges in a point-ion model and the $Q_{\vec{k}j}$ are complex normal coordinates defined by Eq. (26). A transformation to real normal coordinates is effected by

$$Q_{\vec{k}j} = \sqrt{2}\,(q_{\vec{k}j1} + i q_{\vec{k}j2})\,. \tag{45}$$

It is useful to decompose $V_e(r, Q)$ into symmetry-adapted contributions by employing the projection operator[36]

$$P_{\Gamma\gamma} = \frac{d_\Gamma}{g} \sum_R D^{\Gamma *}_{\gamma\gamma}(R) O_R\,, \tag{46}$$

where g is the dimensionality of the symmetry group, d_Γ is the dimensionality of the irreducible representation $D^\Gamma(R)$, and O_R is the rotation operator in wave-vector space. In terms of symmetry-adapted real normal coordinates, the interaction potential is

$$V_{e\phi}(\vec{r}, Q) = \sqrt{2} \sum_{\vec{k}j}^{1/2} \sum_{\lambda=1}^{2} g_{\vec{k}j} \sum_{\Gamma\gamma} q^{\Gamma\gamma}_{\vec{k}j\lambda} P_{\Gamma\gamma} \begin{Bmatrix} \sin(\vec{k}\cdot\vec{r}) \\ \cos(\vec{k}\cdot\vec{r}) \end{Bmatrix}, \tag{47}$$

where $\sin\vec{k}\cdot\vec{r}$ ($\cos\vec{k}\cdot\vec{r}$) applies when $\lambda = 1$ (2). The wave-vector sum is over one-half of the first Brillouin zone. When the defect contains more than a single electron, then a sum over electron coordinates is included.

The single-phonon-sideband line shape associated with the $^2A_2 \leftarrow {}^2E$ transition (R_2 band) accompanied by the creation of single A_1 phonons is, from Eqs. (36) and (37),

$$s_1^{A_1}(\hbar\omega) = (2\hbar^2)^{-1} \sum_{\vec{k}j}^{1/2} \sum_{\lambda=1}^{2} (\Delta V^{A_1}_{\vec{k}j\lambda})^2 \frac{\delta(\omega - \omega_{\vec{k}j})}{\omega^3_{\vec{k}j}}\,, \tag{48}$$

where

$$\Delta V^{A_1}_{\vec{k}j\lambda} \equiv V^{A_1}_{\vec{k}j\lambda}(^2A_2) - V^{A_1}_{\vec{k}j\lambda}(^2E)\,, \tag{49}$$

and

$$V^{A_1}_{\vec{k}j\lambda}(^{2S+1}\Gamma) = \sqrt{2}\, g_{\vec{k}j} \left\langle {}^{2S+1}\Gamma \left| P_{A_1} \sum_{i=1}^{3} \begin{Bmatrix} \sin(\vec{k}\cdot\vec{r}_i) \\ \cos(\vec{k}\cdot\vec{r}_i) \end{Bmatrix} \right| {}^{2S+1}\Gamma \right\rangle . \tag{50}$$

The kets $|^{2S+1}\Gamma\rangle$ represent the R-center electronic states (multiconfigurational) described in I. In practice, the delta function is eliminated by averaging over a finite frequency interval $\Delta\omega$.

The Jahn-Teller parameters are similar in form and describe the coupling between the ^2E ground electronic state and the E-symmetry vibrational modes. The coupling to the $^2A_2$ state vanishes by symmetry. The optical spectrum appropriate to E vibrational modes is characterized by

$$k^2_{\text{eff}} = \hbar^{-1} \sum_{\vec{k}j}^{1/2} \sum_{\lambda=1}^{2} [V^E_{\vec{k}j\lambda}(^2E)]^2/\omega^3_{\vec{k}j}\,, \tag{51}$$

$$\omega_{\text{eff}} = \left(\hbar^{-1} \sum_{\vec{k}j}^{1/2} \sum_{\lambda=1}^{2} [V^E_{\vec{k}j\lambda}(^2E)]^2/\omega^2_{\vec{k}j} \right) \Big/ k^2_{\text{eff}}\,, \tag{52}$$

and

$$\langle\omega^2\rangle = \left(\hbar^{-1} \sum_{\vec{k}j}^{1/2} \sum_{\lambda=1}^{2} [V^E_{\vec{k}j\lambda}(^2E)]^2/\omega_{\vec{k}j} \right) \Big/ k^2_{\text{eff}}\,, \tag{53}$$

where

$$V^E_{\vec{k}j\lambda}(^2E) = \sqrt{2}\, g_{\vec{k}j} \left\langle {}^2E\gamma \left| P_{E\gamma''} \sum_{i=1}^{3} \begin{Bmatrix} \sin(\vec{k}\cdot\vec{r}_i) \\ \cos(\vec{k}\cdot\vec{r}_i) \end{Bmatrix} \right| {}^2E\gamma' \right\rangle \Big/ U^{(\gamma'')}_{\gamma\gamma'} \tag{54}$$

for $U^{(\gamma'')}_{\gamma\gamma'}$ nonvanishing.

The quantities described by Eqs. (48), (51), (52), and (53) were evaluated for the R center in KCl using the appropriate wave functions from I. The set of lattice eigenmodes was extended to include core and shell motions as described in Sec. II; hence, the effects of atomic polarizability are included. It is noted that the R-center functions are defined in a local coordinate system having a z

axis along the [111] direction. Therefore, the wave vectors appearing as arguments of the sine and cosine functions are rotated to the local system.

The calculated single-phonon-sideband line shape $s_1^{A_1}(\omega)$ is shown as a histogram in Fig. 1. This corresponds to a transition from the ^2E ground state to the first $^2A_2$ excited state accompanied by the creation of single A_1 phonons. The corresponding Huang-Rhys factor is 2.62 and represents the area under the curve. The single-phonon-sideband line shape as inferred from optical-absorption measurements is also shown in the figure as a smooth curve. The deconvolution is due to Giesecke *et al.*[4] and has been normalized to a Huang-Rhys factor of 3.5.[3]

The effective coupling constant for E-vibrational modes interacting with the ^2E ground state, k_{eff}^2, is calculated as 5.22. The associated effective frequency ω_{eff} and the second moment, $\langle\omega^2\rangle$ are 25.1×10^{12} sec^{-1} and 6.73×10^{26} sec^{-2}, respectively. For a Gaussian line shape, these correspond to a full width half maximum (FWHM) of 15.4×10^{12} sec^{-1}. The absorption curve associated with the creation of single E-mode phonons is shown in Fig. 2, where it is taken to be Gaussian and normalized to $k_{\text{eff}}^2/2$. The single-phonon-sideband line shape inferred from experiment is also shown in the figure. It is important to note, however, that the deconvolution is rigorously correct only for nondegenerate modes of vibration; hence, this method is only approximate. It is not a bad approximation for the case of an electronic transition to a nondegenerate state and it becomes a good approximation in the strong-coupling limit. A discussion of these results and those for the symmetrical vibrations is presented in Sec. VI.

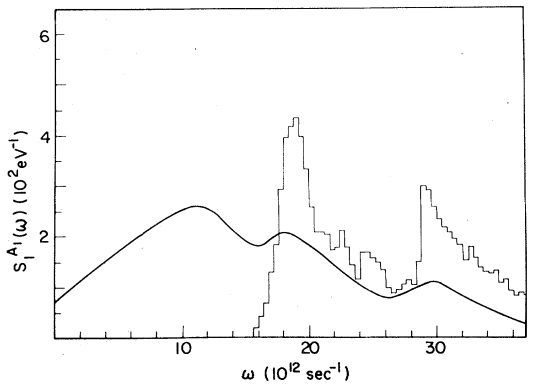

FIG. 1. Single-phonon-sideband line shape for A_1 modes calculated by the Ritter and Markham (Ref. 11) method (histogram) and inferred from experiment (Ref. 4) (smooth curve; see text).

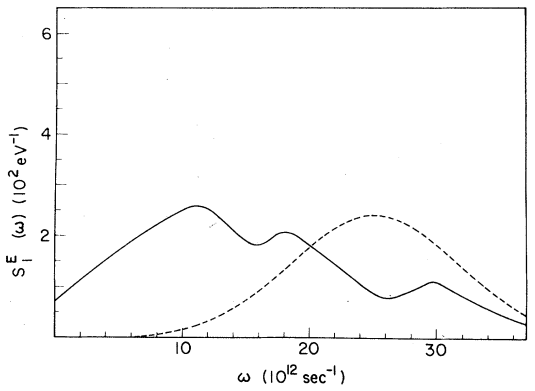

FIG. 2. Single-phonon-sideband line shape for E modes calculated by the Ritter and Markham (Ref. 11) method (dashed line).

V. COMPACT-WAVE-FUNCTION APPROXIMATION FOR OPTICAL-ABSORPTION CALCULATIONS: GREEN'S-FUNCTION APPROACH

The Ritter and Markham[11] approach, described in the preceding section, incorporates a number of approximations. It neglects the details of the electron-lattice coupling in the region near the defect. Also, the normal-lattice spectrum is assumed to be unaltered by the presence of the defect. In the present treatment, an alternative procedure is developed which is not restricted by this set of simplifying assumptions. A transformation from normal coordinates is performed in such a way that each new coordinate is symmetry adapted and denotes a set of ions which are at the same distance from the center of the defect. This method is made tractable by assuming that the change in the coupling constants associated with the electronic transition vanishes for ions beyond a certain distance from the defect. A perturbed-lattice Green's function is generated from Eq. (21) where it is assumed that the change in the force-constant matrix also vanishes outside of this same set of ions.

Equation (36) for the single-phonon sideband $s_1(E)$ may be combined with Eqs. (37) and (28) to obtain

$$s_1(E)=\sum_j(\Delta\underline{F}^{\dagger}\underline{\chi}_j\underline{\chi}_j^{\dagger}\Delta\underline{F}/2\hbar\omega_j^3)\delta(E-\hbar\omega_j)\,, \quad (55)$$

where $\Delta\underline{F}$ is the change in the force vector associated with the transition between electronic states. By analogy with Eq. (11), the imaginary part of the perturbed-lattice Green's-function matrix is given by

$$\mathrm{Im}\underline{G}(\omega^2-i\epsilon)=\frac{\pi\hbar}{2\omega}\sum_j\underline{\chi}_j\underline{\chi}_j^{\dagger}\delta(E-\hbar\omega_j)\,. \quad (56)$$

Both $\underline{G}$ and $\Delta\underline{F}$ may be referred to real, symmetry-adapted combinations of displacements, with concomitant partitioning of $\underline{G}$. Since Eq. (55) is valid only for coupling to modes of A_1 symmetry, we obtain for their contribution to the single-phonon sideband

$$s_1^{A_1}(\hbar\omega)=\frac{1}{\pi\hbar^2\omega^2}\Delta\underline{F}^{A_1\dagger}\mathrm{Im}\{[\underline{I}-\underline{G}^{0A_1}(\omega^2-i\epsilon)\delta\underline{L}^{A_1}]^{-1}\times\underline{G}^{0A_1}(\omega^2-i\epsilon)\}\Delta\underline{F}^{A_1}, \tag{57}$$

where we have exploited Eq. (21). The contribution of A_1 modes to the Huang-Rhys factor S^{A_1} is then given in terms of $s_1^{A_1}(h\omega)$ by Eq. (35). The Jahn-Teller parameters, analogous to those of Eqs. (51), (52), and (53), are given by

$$k_{\mathrm{eff}}^2=\underline{V}^{E\gamma\dagger}\frac{2}{\pi\hbar}\int\mathrm{Im}\{[\underline{I}-\underline{G}^{0E}(\omega^2-i\epsilon)\delta\underline{L}^{E}]^{-1}\times\underline{G}^{0E}(\omega^2-i\epsilon)\}\frac{d\omega}{\omega^2}\underline{V}^{E\gamma'}, \tag{58}$$

$$\omega_{\mathrm{eff}}=\left(\underline{V}^{E\gamma\dagger}\frac{2}{\pi\hbar}\int\mathrm{Im}\{[\underline{I}-\underline{G}^{0E}(\omega^2-i\epsilon)\delta\underline{L}^{E}]^{-1}\times\underline{G}^{0E}(\omega^2-i\epsilon)\}\frac{d\omega}{\omega}\underline{V}^{E\gamma'}\right)\Big/k_{\mathrm{eff}}^2, \tag{59}$$

and

$$\langle\omega^2\rangle=\left(\underline{V}^{E\gamma\dagger}\frac{2}{\pi\hbar}\int\mathrm{Im}\{[\underline{I}-\underline{G}^{0E}(\omega^2-i\epsilon)\delta\underline{L}^{E}]^{-1}\times\underline{G}^{0E}(\omega^2-i\epsilon)\}d\omega\underline{V}^{E\gamma'}\right)\Big/k_{\mathrm{eff}}^2. \tag{60}$$

The coupling constants $\underline{V}^{E\gamma}$ are defined as

$$\underline{V}^{E\gamma}=\frac{\partial}{\partial\underline{u}^{E\gamma}}\langle{}^2E\gamma'|V_{e\phi}(r,u)|{}^2E\gamma''\rangle/U_{\gamma'\gamma''}^{(\gamma)} \tag{61}$$

for $U_{\gamma'\gamma''}^{(\gamma)}$ nonvanishing. The changes in the matrix $\underline{L}$ are symmetrized by averaging over all of the rows of E.

The perfect-lattice Green's function, the static forces, and the changes in the matrix $\underline{L}$ are calculated by the methods described in Sec. II. The calculation of $\delta\underline{L}$ is simplified by freezing the wave function $\psi(r,x)$ appearing in Eq. (18) when the derivatives of Eq. (17) are evaluated; i.e., $\psi(r,x)\simeq\psi(r,x^0)$, where x^0 represents the perfect-lattice conformation. The elements of these vectors and matrices are assumed to be nonvanishing only for the nearest five ions and three vacancies to the geometrical center of the defect.

Before the single-phonon-sideband line shape is evaluated, it is necessary to eliminate the electron-lattice coupling to displacements which represent rigid translations, since displacement of all the ions with respect to the electronic wave function violates the adiabatic approximation. This is accomplished by first effecting a unitary transformation to a new set of symmetry-adapted coordinates with one element representing a rigid translation. The elements of $\underline{V}^{A_1}$ and $\delta\underline{L}^{A_1}$ associated with this displacement are set to zero. The inverse transformation is applied and $s_1^{A_1}(\hbar\omega)$ is now evaluated according to Eq. (57) where the undesired elements are no longer present. A translational coordinate associated with E displacements is eliminated by the same procedure.

The resulting single-phonon-sideband line shape is shown in Fig. 3 for $\delta\underline{L}^{A_1}=0$ and in Fig. 4 for $\delta\underline{L}^{A_1}\neq0$. The first case is appropriate to perfect-lattice modes of vibration. The calculated Huang-Rhys factors for the perfect- and perturbed-lattice cases are 5.14 and 7.45, respectively.

The effective E-mode coupling constants for the perfect- and perturbed-lattice cases are 3.44 and 8.72, respectively. The corresponding effective frequencies are 17.0×10^{12} sec^{-1} and 12.1×10^{12} sec^{-1}, and the second moments are 3.27×10^{26} sec^{-2} and 1.65×10^{26} sec^{-2}. For Gaussian line shapes, the FWHM's are 14.6×10^{12} sec^{-1} and 10.2×10^{12} sec^{-1} (see Fig. 5 and the discussion at the end of Sec. IV). A discussion of these results is presented in Sec. VI.

VI. DISCUSSIONS AND CONCLUSIONS

The point-ion-model wave functions appropriate to a rigid-lattice conformation have been employed in calculations of the optical-absorption line shape for the R_2 band in KCl. The effects of coupling to A_1 modes of vibration are embodied

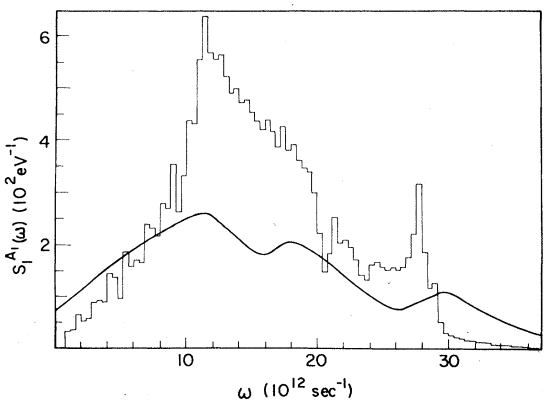

FIG. 3. Single-phonon-sideband line shape for A_1 modes calculated by the Green's-function method ($\delta\underline{L}^{A_1}=0$).

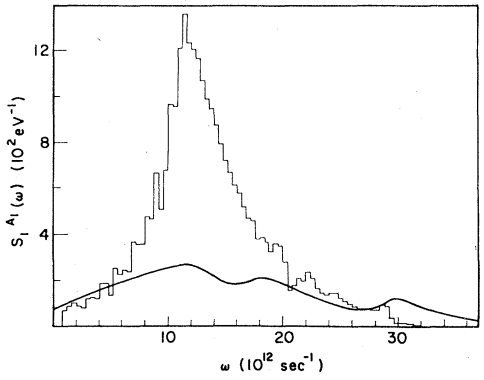

FIG. 4. Single-phonon-sideband line shape for A_1 modes calculated by the Green's-function method ($\delta \underline{L}^{A_1} \neq 0$).

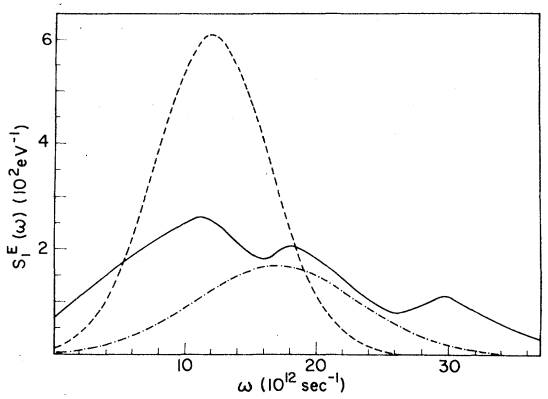

FIG. 5. Single-phonon-sideband line shape for E modes calculated by the Green's-function method (—·—·— for $\delta \underline{L}^E = 0$ and --- for $\delta \underline{L}^E \neq 0$).

in the single-phonon-sideband line shapes, $s_1^{A_1}(\hbar\omega)$, shown in Figs. 1, 3, and 4. Comparisons are made to $s_1(\hbar\omega)$ as inferred from experiment.[3,4] The corresponding Huang-Rhys factors are contained in Table I. The Jahn-Teller parameters, k_{eff}^2, ω_{eff}, and $\langle\omega^2\rangle$, which characterize the optical absorption associated with E modes of vibration, are also summarized in Table 1. The corresponding single-phonon-sideband line shapes are shown in Figs. 2 and 5.

The single-phonon-sideband line shape as calculated in the diffuse-wave-function approximation (Fig. 1) is seen to agree quite well with experiment at higher frequencies. This procedure gives no contribution to $s_1^{A_1}(\hbar\omega)$ at lower frequencies. It seems that the detailed nature of the electron-lattice coupling which occurs near the defect is important in the low-frequency region. These effects are neglected entirely in the diffuse-wave-function, or Ritter and Markham,[11] approximation.

The best results in the compact-wave function, or Green's-function, approximation are obtained when only perfect-lattice modes of vibration are considered (Fig. 3). In this case, the low-frequency contributions to $s_1^{A_1}(\hbar\omega)$ are predicted, but the high-frequency results are not as good as those from the diffuse-wave-function approximation. This is an expected behavior since this procedure treats the details of the coupling near the defect quite well, while ignoring these beyond a certain distance. The overall agreement is good in view of the approximations made.

A problem is seen to arise when the force-constant matrix is altered to account for the presence of the defect, especially the vacancies. The reduction of the force constants leads to an enhanced absorption at low frequencies (Fig. 4). These results indicate that the electron-lattice coupling constants are somewhat too large and therefore that the wave functions are too compact. A reduction in $s_1^{A_1}(\hbar\omega)$ would be expected if extended-ion effects and lattice relaxation were included. This is consistent with the conclusions drawn from I.

The effective coupling constant k_{eff}^2 has been calculated by the three methods mentioned above (Table I). They are in fair agreement with the empirical values listed in Table IX of I, although somewhat larger. This discrepancy is also attributable to excessively compact wave functions.

The effective frequencies calculated by all of

TABLE I. Optical-absorption parameters in the diffuse- and compact-wave-function approximations. The units of ω_{eff} and FWHM are 10^{12} sec^{-1}, and $\langle\omega^2\rangle$ is in units of 10^{26} sec^{-2}.

Lattice dynamics	S^{A_1}	k_{eff}^2	ω_{eff}	$\langle\omega^2\rangle$	FWHM
Diffuse-wave-function approximation: Ritter and Markham approach					
Perfect	2.62	5.22	25.1	6.73	15.4
Compact-wave-function approximation: Green's-function approach					
Perfect	5.14	3.44	17.0	3.27	14.6
Perturbed	7.45	8.72	12.1	1.65	10.2

these methods fall between the first and third peaks in the empirical line-shape curves (Figs. 2 and 5). This is quite satisfying since MCD studies[37,38] have demonstrated that E-mode absorption is associated with the second absorption peak. If A_1 modes are assumed to be absent and a Gaussian line shape is used to describe the single-phonon-sideband, then the FWHM's would be given by the values listed in Table I. Inspection of the absorption curves associated with the second peak in Figs. 2 and 5 reveals that the line shape appropriate to the perfect-lattice Green's-function approach agrees most closely with experiment.

In summary, *ab initio* calculations of the R_2-band line shape, using detailed electronic wave functions, are in reasonable agreement with experiment. The Ritter-Markham and Green's-function methods appear to have complimentary deficiencies. Finally, incorporation of ion-size and lattice-relaxation effects would yield a more diffuse wave function and improve agreement with experiment.

ACKNOWLEDGMENTS

The authors would like to thank the Computer Center at the University of Connecticut for the generous amount of computer time which was made available. One of us (G.G.D.) would like to thank Professor D. Markowitz for helpful discussions during the course of this investigation. This work was supported, in part, by NSF Grant No. DMR74-02604.

---

*Based on work submitted in partial fulfillment of the requirements for a Ph.D. in Physics at the University of Connecticut by G. G. DeLeo (1979) and R. C. Kern (1972).

†Permanent address: Department of Physics, Lehigh University, Bethlehem, PA 18015.

‡Permanent address: Nuclear Associates International, Rockville, MD 20852.

[1]C. Z. Van Doorn, Philips Res. Rep. 12, 309 (1957).

[2]R. C. Kern, G. G. DeLeo, and R. H. Bartram, preceding article Phys. Rev. B 24, 2211 (1981).

[3]D. B. Fitchen, R. H. Silsbee, T. A. Fulton, and E. L. Wolf, Phys. Rev. Letters 11, 275 (1963).

[4]P. Giesecke, W. von der Osten, and U. Röder, Phys. Status Solidi B 51, 723 (1972).

[5]M. H. L. Pryce, in *Phonons in Perfect Lattices and Lattices with Point Imperfections*, edited by R. W. H. Stevenson (Oliver & Boyd, Edinburgh, 1966), p. 403.

[6]U. Schröder, Solid State Commun. 4, 347 (1966).

[7]R. C. O'Rourke, Phys. Rev. 91, 265 (1953).

[8]M. C. M. O'Brien, J. Phys. C 5, 2045 (1972).

[9]A. D. Liehr and W. Moffitt, J. Chem. Phys. 25, 1074 (1956).

[10]H. C. Longuet-Higgins, U. Öpik, M. H. L. Pryce, F. R. S. and R. A. Sack, Proc. R. Soc. London A224, 1 (1958).

[11]J. T. Ritter and J. J. Markham, Phys. Rev. 185, 1201 (1969).

[12]A. A. Maradudin, in *Solid State Physics*, edited by F. Seitz and D. Turnbull (Academic, New York, 1966), Vol. 18, p. 273.

[13]A. A. Maradudin, E. W. Montroll, G. H. Weiss, and I. P. Ipatova, *Theory of Lattice Dynamics in the Harmonic Approximation* (Academic, New York, 1971).

[14]B. G. Dick and A. W. Overhauser, Phys. Rev. 112, 90 (1958).

[15]J. R. D. Copley, R. W. MacPherson, and T. Timusk, Phys. Rev. 182, 965 (1969).

[16]J. B. Page, Jr., and D. Strauch, Phys. Status Solidi 24, 469 (1967).

[17]M. Born and J. E. Mayer, Z. Phys. 75, 1 (1932).

[18]M. P. Tosi, in *Solid State Physics*, edited by F. Seitz and D. Turnbull (Academic, New York, 1964), Vol. 16, p. 1.

[19]K. Huang and A. Rhys, Proc. R. Soc. London A204, 406 (1950).

[20]M. Lax, J. Chem. Phys. 20, 1752 (1952).

[21]R. Kubo and Y. Toyozawa, Prog. Theor. Phys. 13, 160 (1955).

[22]D. E. McCumber, Phys. Rev. 135, A1676 (1964).

[23]T. H. Keil, Phys. Rev. 140, A601 (1965).

[24]W. H. Fonger and C. W. Struck, J. Chem. Phys. 60, 1994 (1974).

[25]G. Arfken, *Mathematical Methods for Physicists*, 2nd ed. (Academic, New York, 1970), p. 681.

[26]R. H. Silsbee, Phys. Rev. 138, A180 (1965).

[27]R. Englman, *The Jahn-Teller Effect in Molecules and Crystals* (Wiley-Interscience, New York, 1972).

[28]J. C. Sloncjewski, Phys. Rev. 131, 1596 (1963).

[29]Y. Toyozawa and M. Inoue, J. Phys. Soc. Jpn. 21, 1663 (1966).

[30]K. Cho, J. Phys. Soc. Jpn. 25, 1372 (1968).

[31]J. R. Fletcher, J. Phys. C 5, 852 (1972).

[32]E. Mulazzi and N. Terzi, Phys. Rev. B 10, 3552 (1974).

[33]Yu. B. Rozenfel'd and V. Z. Polinger, Zh. Eksp. Teor. Fiz. 70, 597 (1976) [Sov. Phys.—JETP 43, 310 (1976)].

[34]M. C. M. O'Brien and S. N. Evangelou, J. Phys. C 13, 611 (1980).

[35]F. S. Ham, in *Electron Paramagnetic Resonance*, edited by S. Geschwind (Plenum, New York, 1972), pp. 1–119.

[36]M. Tinkham, *Group Theory and Quantum Mechanics* (McGraw-Hill, New York, 1964), p. 40.

[37]I. W. Shepherd, Phys. Rev. 165, 985 (1968).

[38]W. Burke, Phys. Rev. 172, 866 (1968).